Results in Physics 8 (2018) 99–103

Contents lists available at ScienceDirect

Results in Physics

journal homepage: www.journals.elsevier.com/results-in-physics

Luminescence in microcrystalline green emitting $Li_2Mg_{1-x}ZrO_4:xTb^{3+}$ $(0.1 \leq x \leq 2.0)$ phosphor

V.R. Panse [a], N.S. Kokode [a], K.N. Shinde [b,*], S.J. Dhoble [c]

[a] N.H. College, Bramhapuri 441206, India
[b] N.S. Science and Arts College, Bhadrawati 442902, India
[c] Department of Physics, RTM Nagpur University, Nagpur 440033, India

ARTICLE INFO

Article history:
Received 5 April 2017
Received in revised form 8 October 2017
Accepted 9 October 2017
Available online 18 October 2017

Keywords:
Photoluminescence
Phosphor
Wet chemical method
Solid state lighting
XRD
SEM

ABSTRACT

Green emitting $Li_2Mg_{1-x}ZrO_4:xTb^{3+}$ $(0.1 \leq x \leq 2.0)$ phosphor powders were synthesized via the wet chemical synthesis and the luminescent proprieties were studied when excited at 380 nm and present a dominant and strong green luminescence peak at 543 nm, due to D–F transition. The preparation of $Li_2Mg_{1-x}ZrO_4:xTb^{3+}$ $(0.1 \leq x \leq 2.0)$ phosphor powders were confirmed by X-ray diffraction (XRD) results without any secondary or impurity phases. The size and morphology of the $Li_2Mg_{1-x}ZrO_4:xTb^{3+}$ $(0.1 \leq x \leq 2.0)$ phosphor powders were further examined by scanning electron microscopy (SEM). Photoluminescence (PL) results have shown strongest green emission at 543 nm, which is originated due to $^5D_4$–$^7F_5$ transition of Tb^{3+} ion, for the $Li_2Mg_{1-x}ZrO_4:xTb^{3+}$ $(0.1 \leq x \leq 2.0)$ phosphor. The addition of concentration Tb^{3+} was greatly improved the photoluminescence properties of present phosphors. The present study suggests that the $Li_2Mg_{1-x}ZrO_4:xTb^{3+}$ $(0.1 \leq x \leq 2.0)$ phosphor is a strong candidate as a green component for phosphor-converted white light-emitting diodes (LEDs).

Introduction

Phosphors are usually made from a suitable host material with an added activator i.e., lanthanide have attracted great attention because of their excellent luminescent properties and consequent applications in lasers, lighting, displays, lasers, scintillators, light-emitting diodes (LED), detectors for X-ray imaging, electroluminescent devices, and solar concentrators [1–3]. Generally host materials, such as nitrides, oxides, sulfides, etc., should possess good optical, mechanical and thermal properties [1]. Activators such as rare earth (RE) metal possess unique optical behavior when doped into host material. The luminescence of these ions is attributed to the electronic transitions occurring within the partially filled 4f energy shell of the lanthanide series [2]. Energy transfer from host material to activators can play an important role in phosphor materials as it can be used to enhance the luminescence efficiency [1]. The remarkable narrow-band emission properties of Eu^{3+}, Tb^{3+}, Dy^{3+} and Tm^{3+} ions have been utilized in the development of efficient phosphors [4]. In particular, Tb ions are used as the activator because their bright green emission is suitable for many applications [1]. This is due to their intense $^5D_4$–$^7F_5$ emission in the green spectral region. Efficiency of a prepared phosphor material mainly depends on a host material and synthesis techniques. In crystal lattice structure an extremely good homogeneity of the prepared phosphor material is required for high efficient Tb^{3+}doped phosphors [5]. Traditionally, RE-doped phosphors were prepared by the solid-state reaction method, which demands longer reaction times and higher annealing temperatures [6]. Today, low temperature methods such as sol–gel [7,8], co-precipitation [9,10], combustion [11] and hydrothermal microwave [12], are used to prepare these phosphors. However, the one-step wet chemical synthesis to prepare the phosphor is very simple, safe, energy saving and takes less time. This synthesis technique has been extensively applied to the preparation of various materials. This method is relatively cost-effective, quick and can be easily exploited to prepare phosphors with enhanced optical properties. The intention of this work is to report our investigation results on the synthesis, surface morphology, photoluminescence and color chromaticity of the new green $Li_2Mg_{1-x}ZrO_4:xTb^{3+}$ $(0.1 \leq x \leq 2.0)$ phosphor powder and their corresponding spectroscopic properties under UV excitation.

Experimental

For preparing the microcrystalline $Li_2Mg_{1-x}ZrO_4:xTb^{3+}$ $(0.1 \leq x \leq 2.0)$ phosphor powder, the simple, one step, wet chemical

* Corresponding author.
E-mail address: kartik_shinde@rediffmail.com (K.N. Shinde).

https://doi.org/10.1016/j.rinp.2017.10.025
2211-3797/

method is used. The starting materials were $LiNO_3$ (Merck 99.99%), $Mg(NO)_2$ (Merck 99.99%), $Zr(NO_3)_4$ (Merck 99.99%), and terbium (III) oxide Tb_4O_7 (Merck 99.99%), double distilled water were used in this study without further purification. Diluted nitric acid is used to convert Tb_4O_7 to terbium nitrate with appropriate ratio.

To synthesized Li_2MgZrO_4:Tb^{3+} phosphor the above chemical reagents treated as raw material in the preferred ratio and dissolved separately in double distilled de-ionized water with the help of magnetic stirrer. After that mix all the dissolved solvent in one beaker, and same for the each concentration and mix them again with the help of magnetic stirrer. All the concentration with the host material is kept in oven for 80 °C for 12 h. Subsequently, the products were gradually cooled to room temperature by switching off the oven and ground into powders for subsequent analysis.

To check the phase purity and structure, the X-ray diffraction (XRD) patterns studied of the prepared host material by using PAN analytical diffratometer with Cu Kα radiation (1.5405 Å) operating voltage at 40 kV, 30 mA and scan step time at 10.3377 s. The morphological behavior of the host material powder was recorded by field-emission scanning electron microscope (JSM-6700 F, JEOL Japan). Photoluminescence spectra i.e., emission and excitation was recorded with the help of RF5301, with the spectral slit of 1.5 nm. The Chromaticity behavior is studied with the help of CIE diagram. All the characterization was done at room temperature and the same amount of samples were taken during each measurement.

Results and discussion

XRD characterization

The representative X-ray diffraction patterns of as-prepared Li_2MgZrO_4 matched well with standard JCPDS file (JCPDS card number 78-0198) of Li_2MgZrO_4. It is observed clearly that no noticeable impurity phase was presented in our synthesized Li_2MgZrO_4 pattern. This suggests that the phosphor samples were well-synthesized by the one step wet chemical method. The XRD pattern of the prepared phosphor is shown in the Fig. 1. Previously, Castellanos et al. reported that the material is crystallized in cubic rock-salt structure of space group Fm square3m [13]. Apart from this, in our case a couple of new diffraction peaks also appear i.e., at 22.5 and 32.7 (2θ degree) which are characteristic diffraction peaks for the prepared samples, but cannot be attributed to any known compounds. These results mean that the synthesized phosphor powders are not the simple physical mixtures of starting materials, but a new single-host Li_2MgZrO_4. The detailed structure of is still under investigation.

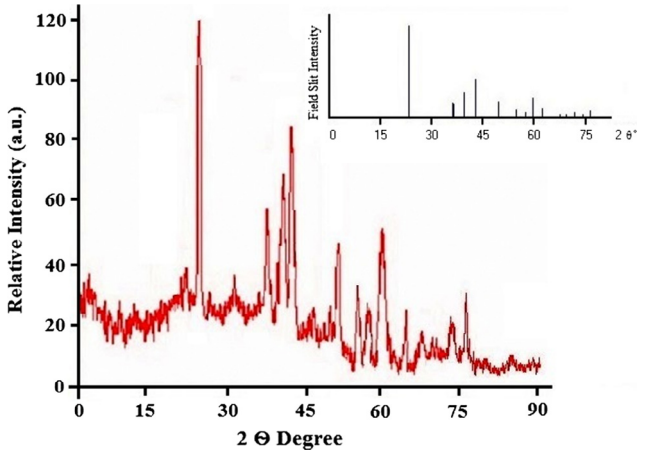

Fig. 1. X-ray diffraction pattern of Li_2MgZrO_4 phosphor powder.

Scanning electron microscopy

We prepared high-quality $Li_2Mg_{1-x}ZrO_4$:xTb^{3+} ($0.1 \leq x \leq 2.0$) phosphor powder by one step, wet chemical method i.e., irregular and spongy type morphologies as well as smooth surfaces. We get the detailed information about the size and shape of the particle from SEM analysis. In spite of the annealing treatment, the powders showed high-quality characteristics. It was found that there are agglomerates and clusters of several particles. It is understandable that in a clustered particle there are many crystalline particles. The particle sizes of Li_2MgZrO_4 powder is in the range of 2–5 μm. The SEM images of prepared material were shown in the Fig. 2. Furthermore, the samples are agglomerated and showing an irregular, foam like morphology. The surface morphology of the Li_2MgZrO_4 powder was not much different from each other, but the particle size is in between from 2 μm to 5 μm.

Optical properties of $Li_2Mg_{1-x}ZrO_4$:xTb^{3+} ($0.1 \leq x \leq 2.0$) phosphor

A series of green emitting microcrystalline $Li_2Mg_{1-x}ZrO_4$:xTb^{3+} ($0.1 \leq x \leq 2.0$) phosphor prepared by simple one step, wet chemical method to study their photoluminescence properties. The excitation spectrum is a combination of a broad band and several narrow peaks. The excitation spectrum of the Li_2MgZrO_4:Tb^{3+} phosphor for monitoring 543 nm at room temperature is given in Fig. 3. It can be seen that the excitation spectrum consists of broad bands in the range from 270 to 300 nm correspond to the strong $4f^75d^1$ absorbability and a series of sharp lines (305, 319, 343,354, 371,375 and 380 nm) in the range from 300 to 400 nm correspond to the weak 4f → 4f absorbability [14,15]. It can be seen that the excitation spectrum are composed of several sharp bands, including the bands at 305 nm ($^7F_6 \rightarrow {}^3H_6$), 319 nm ($^7F_6 \rightarrow {}^5D_0$), 343 nm ($^7F_6 \rightarrow {}^5L_7$), 354 nm ($^7F_6 \rightarrow {}^5L_9$), 371 nm ($^7F_6 \rightarrow {}^5G_5$), and 380 nm ($^7F_6 \rightarrow {}^5G_6$). These sharp lines represent the spin-forbidden 4f–4f transitions [15–17]. The band peaking at 284 nm represents the spin allowed 4f–5d transition (f–d transition) of Tb^{3+} ions [18]. All the excitation intensities increase with an addition of the Tb^{3+} content and reach the maximum when Tb^{3+} ions are 2 Mol%. Here, in Fig. 3, we shown only optimum concentration i.e., $x = 2$ Mol% for better understanding. The position of the excitation peak is not influenced by the Tb^{3+} concentration. However, the excitation intensity increases with increase in Tb^{3+} concentration and reaches the maximum at about 2 Mol%.

The emission spectrum recorded under the 380 nm excitation is shown in Fig. 4. A noticeable change in emission position is observed by changing the Tb^{3+} content. As shown in Fig. 4, all the $Li_2Mg_{1-x}ZrO_4$:xTb^{3+} ($0.1 \leq x \leq 2.0$) phosphors emitted the light wavelength near yellowish green light, approximating a green luminescence with a peak wavelength of 543 nm. The emission spectrum exhibits major emission peak at around 543 nm, which is attributed to the typical $^5D_4 \rightarrow {}^7F_5$ transition of Tb^{3+} ions [14]. The emission spectra excited under 380 nm consist of several peaks centered at 488, 543, 583 and 625 nm, which result from the $^5D_4 \rightarrow {}^7F_J$ ($J = 6, 5, 4$, and 3) transitions of Tb^{3+}, respectively. Among these peaks, the green emission peak ($^5D_4 \rightarrow {}^7F_5$) located at 545 nm is the most dominant, which is favorable for obtaining a phosphor with high color purity [19].

These typical emission peaks are split in different ways. The energy level $^5D_4 \rightarrow {}^7F_4$ transition is split into 543 and 550 nm emission peaks and $^5D_4 \rightarrow {}^7F_4$ transition is split into 582 and 589 nm emission peaks [14]. These splits were related to in the crystal field effect which resemblance with reported by Li et al. [14] in the case of $LiBaBO_3$:Tb^{3+} phosphor. Among these transitions, the green

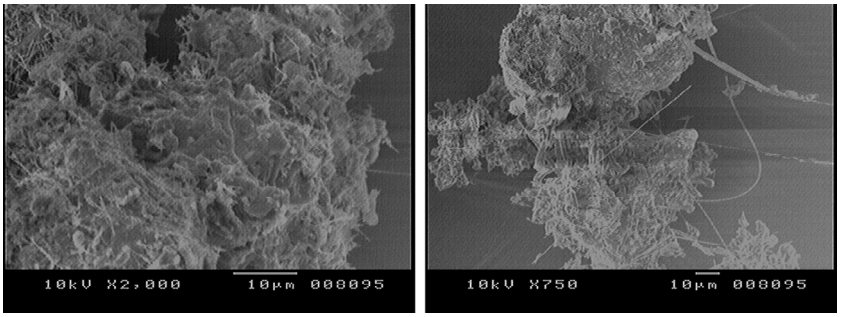

Fig. 2. SEM images of Li_2MgZrO_4 Phosphor.

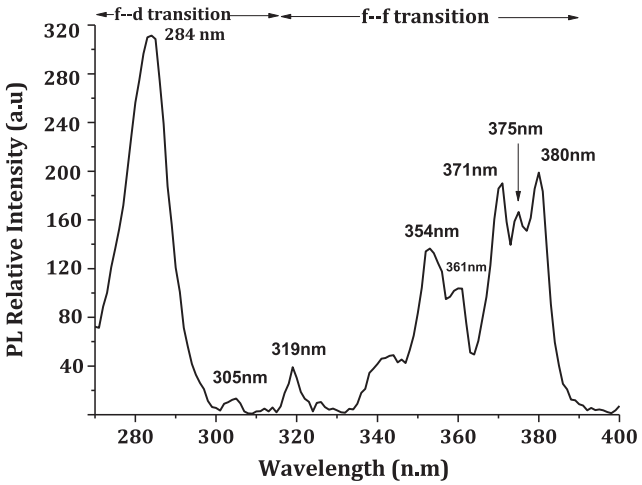

Fig. 3. Excitation Spectrum of Li_2MgZrO_4:Tb^{3+} phosphor monitored at 543 nm.

emission at 543 nm ($^5D_4 \rightarrow {}^7F_5$) is the most intense. The emission intensity depends strongly on the content of the Tb^{3+} ions. Under the 380 nm excitation, all the samples with different doping content of Tb^{3+} display the similar emission spectra except for emission intensity.

Furthermore, the fundamental relationship between Tb^{3+} concentration and PL intensity of $Li_2Mg_{1-x}ZrO_4$:xTb^{3+} ($0.1 \leq x \leq 2.0$) phosphor under 380 nm excitations is shown in Fig. 5. Since PL emission intensity strongly depends on both activator concentrations and excitation energy, the action of the exciting carriers to activator ions can be studied by measuring the intensity of the activator luminescence as a function of either activator concentration with constant excitation energy, or excitation energy with a constant activator concentration [20]. Clearly, from Fig. 5 shows that the most intense peak is observed at $x = 2.0$ due to the larger number of luminescent centers and then the intensities decreased slightly, owing to the energy transfer between the neighboring Tb^{3+} ions, i.e., quenching of the emission of Tb^{3+} [21]. At above $x = 2.0$ concentration, the excitation energy transferred in the Mg^{2+} sublattice might be lost on some defect sites or captured by some impurities, resulting in the decrease of the emission intensity of Tb^{3+}.

Energy level diagram

Fig. 6 depicts an energy level showing the transition of Tb^{3+} ions and the luminescence process. All the emission peaks peaking at 488, 543, 583, and 625 nm are obtained from the transitions from the energy level $^5D_4$ to ^5F_J ($J = 6$, 5, 4, and 3) of Tb^{3+} ions, respectively.

According to this mechanism, Tb^{3+} ions are first excited from the ground state to the excited state $^5D_2$, drop down non-radiatively to the excited level $^5D_4$, and finally fall down radiatively to the various energy levels of ^7F_J ($J = 6$–3) [19,22] It is considered that the $Li_2Mg_{1-x}ZrO_4$:xTb^{3+} ($0.1 \leq x \leq 2.0$) can be potential green-emitting phosphor for near ultraviolet excited light emitting

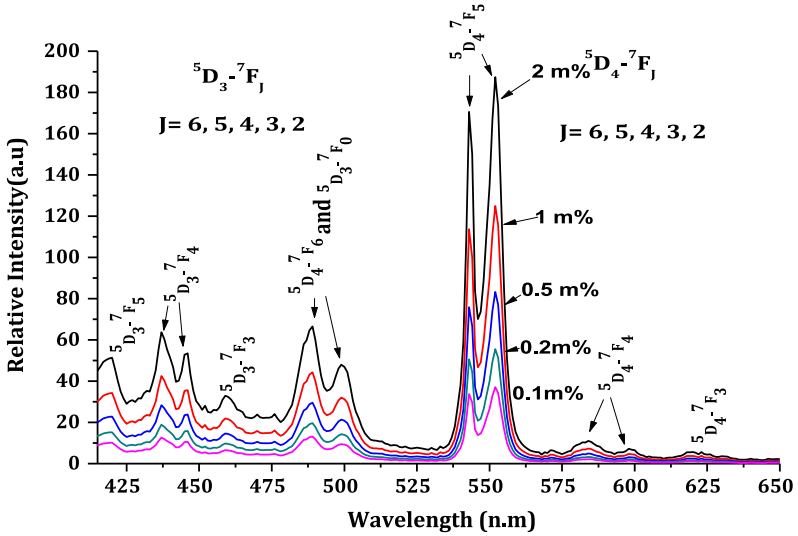

Fig. 4. Emission Spectra of $Li_2Mg_{1-x}ZrO_4$:xTb^{3+} ($0.1 \leq x \leq 2.0$) phosphor when excited at 380 nm.

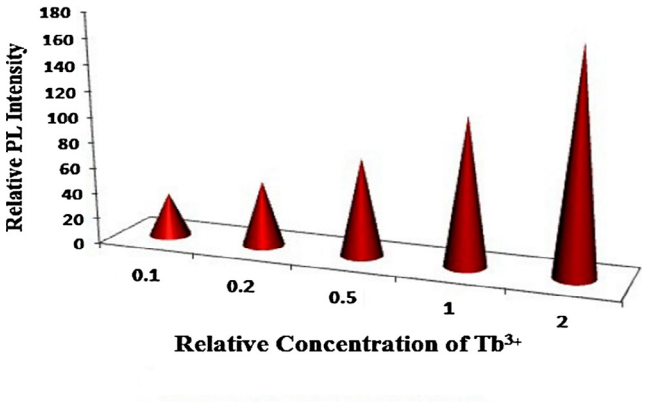

Fig. 5. Concentration dependence of relative emission intensity of $Li_2Mg_{1-x}ZrO_4$: xTb^{3+} ($0.1 \leq x \leq 2.0$) phosphor.

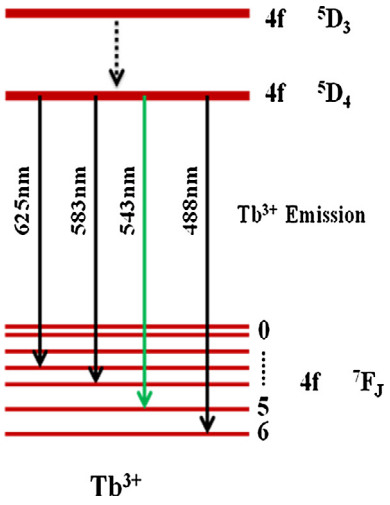

Fig. 6. A schematic diagram showing the transition of Tb^{3+} ions in $Li_2Mg_{1-x}ZrO_4$: xTb^{3+} ($0.1 \leq x \leq 2.0$) phosphor and the luminescence process.

diodes used as a green emitting phosphor for white light emitting diodes and various photonic applications.

Chromaticity nature

Fig. 7 shows the CIE chromaticity diagram for $Li_2Mg_{1-x}ZrO_4$: xTb^{3+} ($0.1 \leq x \leq 2.0$) phosphor excited at 380 nm. The green emission color coordinates in the present experiment study of prepared Li_2MgZrO_4:Tb^{3+} phosphor and calculated from the corresponding emission and excitation spectra. In general, the color of any light source can be represented on the (x, y) coordinate in this color space. The color purity was compared to the 1931 CIE Standard Source C (illuminant Cs (0.3101, 0.3162)). In the present investigation, the chromatic coordinates (x, y), was calculated using the color calculator program radiant imaging [23,24]. The coordinates of the $Li_2Mg_{1-x}ZrO_4$:xTb^{3+} ($0.1 \leq x \leq 2.0$) phosphor of color green ($x \approx 0.256$, $y \approx 0.731$). All the results calculated from the emission spectra are plotted in the *Commission Internationale del' Eclairage* (CIE) 1931 chromaticity diagram, as shown in Fig. 7. It indicates that Tb^{3+} doped $Li_2Mg_{1-x}ZrO_4$ is close to the edge of CIE diagram, which indicates the high color purity of this phosphor.

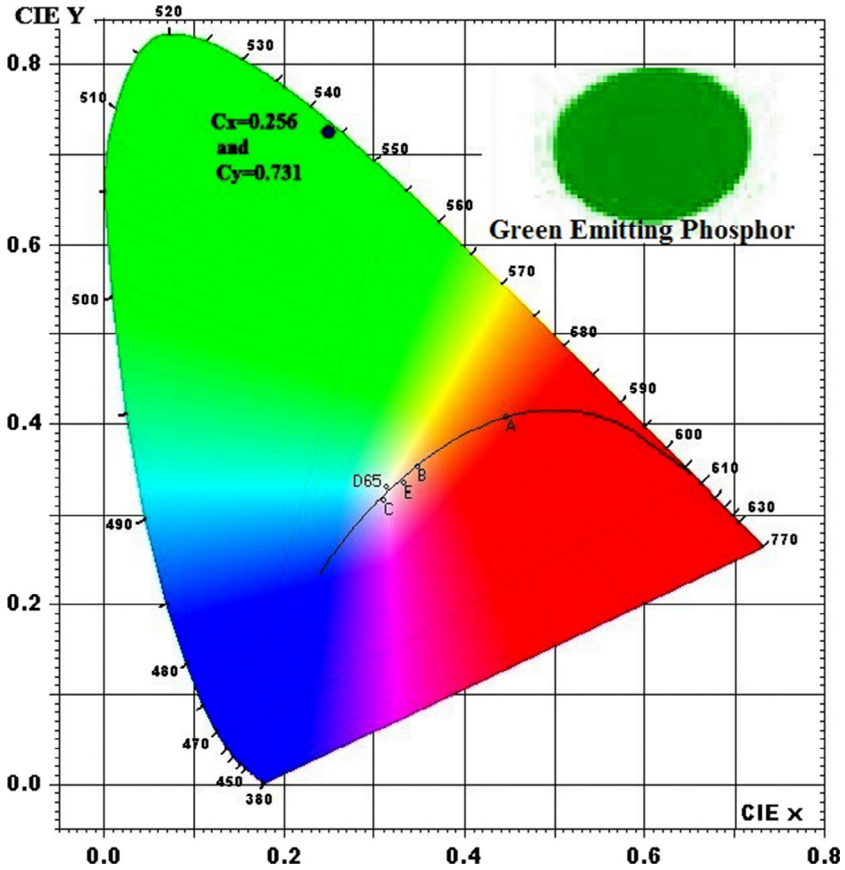

Fig. 7. CIE chromatic diagram showing the chromatic coordinates for $Li_2Mg_{1-x}ZrO_4$:xTb^{3+} ($0.1 \leq x \leq 2.0$) phosphor.

Conclusions

In summary, a series of novel $Li_2Mg_{1-x}ZrO_4:xTb^{3+}$ ($0.1 \leq x \leq 2.0$) phosphor green emitting phosphor was successfully synthesized by the homogeneous and simple wet chemical method at 80 °C for 12 h and their luminescence properties were investigated. The particle size of prepared sample is in sub micrometer range and possesses irregular, foam like morphology.

The luminescence intensity of $Li_2Mg_{1-x}ZrO_4:xTb^{3+}$ ($0.1 \leq x \leq 2.0$) phosphor can be significantly improved by doping an appropriate amount of Tb^{3+} and the luminescence color is stable. The PL spectra show the strongest emission at 543 nm corresponding to the $^5D_4$–$^7F_5$ transition of Tb^{3+} in present phosphor. It is shown that 2.0 Mol% of the doping concentration of Tb^{3+} ions in Li_2MgZrO_4 phosphor under 380 nm excitation is optimum. Such morphology, high luminescence intensity, color purity, and stability are very useful for practical application in the field of photonics. Much characterization analysis will need to be evaluated in future studies. These are under development and will be reported in the near future. Strong absorption in deep NUV region for $Li_2MgZrO_4:Tb^{3+}$ (2.0 Mol%) phosphor suggests that it can have important luminescent applications. Thus, Li_2MgZrO_4: Tb^{3+} (2.0 Mol%) phosphor material presents very attractive luminescent property for the generation of the green color.

Acknowledgement

One of the authors SJD is grateful to Director, Inter-University Accelerator Centre (IUAC), New Delhi, for providing financial assistance to carry out this work under the research project.

References

[1] Seed Ahmed HAA, Ntwaeaborwa OM, Kroon RE. J Lumin 2013;135:15–9.
[2] Gedam SC, Dhoble SJ, Moharil SV. J Lumin 2007;126:121–9.
[3] Llanos Jaime, Castillo Rodrigo. J Lumin 2010;130:1124–7.
[4] Natarajan V, Dhobale AR. J Lumin 2009;129:290–3.
[5] Zhou Li-Ya, Weia Jian-She, Shib Jian-Xin, Gongb Meng-Lian, Liang Hong-Bin. J Lumin 2008;128:1262–6.
[6] Shinde KN, Dhoble SJ. Micro Nano Lett 2010;5(5):340–2.
[7] Rao RP. J Lumin 2005;113:271–8.
[8] Briche S, Zambon D, Boyer D, Chadeyron G, Mahiou R. Opt Mater 2006;28:615–20.
[9] Riwotzki K, Haase M. J Phys Chem B 1998;102:10129–35.
[10] Yan B, Gu J. J Non-Cryst Solids 2009;355:826–9.
[11] Arul Dhas N, Patil KC. J Alloys Compd 1993;202:137–41.
[12] Byrappa K, Yoshimura M. Handbook of Hydrothermal Technology. William Andrew Publishing LLC.; 2001. pp. 754–814.
[13] Castellanos M, West AR, Reid WB. Acta Cryst 1985;C41:1707–9.
[14] Li P, Pang L, Wang Z, Yang Z, Guo Q. Xu Li. J Alloys Compds 2009;478:813–5.
[15] Liu Y, Yang Z. Mater Lett 2011;65:1853–5.
[16] Zhou LY, Choy WCH, Shi JX, Gong ML, Liang HB. Mater Chem Phys 2006;100:372–4.
[17] Wang R, Xu J, Chen C. Mater Lett 2012;68:307–9.
[18] Singh V, Watanabe S, Gundu Rao TK, Al-Shamery Katharina, Haase Markus, Jho Young-Dahl. J Lumin 2012;132:2036–42.
[19] Shinde KN, Dhoble SJ, Yoon SJ, Park K. J Nanosci Nanotechnol 2014;14(8):5957–60.
[20] Ren Zhouyun, Tao Chunyan, Yang Hua, Feng Shouhua. Mat Lett 2007;61:1654–7.
[21] Weng M, Yang R, Peng Y, Chen J. Ceram Int 2012;38:1319–23.
[22] Zhu L, Lu A, Zuo C, Shen W. J Alloys Compd 2011;509:7789–93.
[23] Dhoble SJ, Pawade VB, Shinde KN. Eur Phys J Appl Phys 2010;52. 11104p1–11104p10.
[24] Color Calculator version 2, A software from Radiant Imaging, Inc.; 2007.